Numerical analysis of a smeared cracking model for concrete structures

Eduarda M. Ferreira[1], Flávio S. Barbosa[1], George O. Ainsworth Junior[1]

[1]*Graduation Program in Civil Engineering, Federal University of Juiz de Fora*
University Campus, Engineering College, 36036-330, Juiz de Fora, Brazil
eduarda.marques@engenharia.ufjf.br, flavio.barbosa@engenharia.ufjf.br, george.ainsworth@engenharia.ufjf.br

Abstract. Analytical models for concrete often become ineffective or difficult to parameterize due to its highly complex and heterogeneous microstructure, as well as its physically non-linear behavior. This fact justifies the use of numerical methods, such as the Finite Element Method, for modeling the mechanical behavior of the material more realistically. One of the main phenomena responsible for the physical nonlinearity of concrete is cracking, which occurs even at low loading levels, due to its low tensile strength when compared to the compressive one. In this context, the present work aims to study cracked concrete structures using a smeared cracking model based on monitoring the deterioration of the material's physical properties. The Finite Element model was implemented using an isoparametric element for plane elasticity. The cracking process is described by the decay of stresses with increased strains, through different stress-strain relationships extracted from the literature that represents the overall behavior of concrete in tension or compression. A cracking model based on the inversion of compliance with a local secant constitutive matrix was used, which takes into account the undamaged secant Young's modulus of the material. This nonlinear model has been implemented using the MatLab platform with a generalized displacement control sover. The results for different combinations of stress-strain curves were compared and the method was validated through comparison with the ones of other authors.

Keywords: Finite Element Analysis, Smeared Crack, Concrete Structures

1 Introduction

Concrete is a material widely used in structures, which may be due to its low cost, easy access, and good mechanical performance. However, in general, concrete structures require elaborate constitutive models for their study. Because it is a heterogeneous material with physically non-linear behavior, analytical models for concrete are often difficult to formulate and solve. In this context, the use of numerical methods, such as the finite element method, facilitates the modeling of the mechanical behavior of concrete.

Compared to the compressive strength, the tensile strength is lower, and this fact is fundamental in the characterization of concrete mechanical behavior. Due to this, cracks could appear even at low load stages. In the numerical simulation of cracked concrete structures by the finite element method usually three models are used to represent the cracks: discrete, smeared, and embedded.

In discrete crack models, the mesh needs to be redefined when crack formation occurs. The cracks are inserted along the edges of the elements of the original mesh, generating discontinuities in the displacement field. Pioneering work in this sense is the one by Ngo and Scordelis [1], who presented a discrete model for reinforced concrete where the cracks were inserted in the mesh according to empirical patterns from the duplication of the nodes of the elements. More recently, a noticeable work by Manzoli et al. [2] presented a technique of mesh fragmentation and the introduction of solid interface elements with a high aspect ratio between the elements of the mesh.

In smeared crack models, the cracked material is modeled as continuous, and the cracking process causes changes in the constitutive relations of the finite elements. In 1968, Rashid [3] presented a simplified model that already applied characteristics of current smeared cracking models, such as changing the material's mechanical properties in damaged regions. A few years later, Suidan and Schnobrich [4] presented a model that maintains a transverse residual stiffness, reducing the initial shear modulus through a shear retention factor, in contrast to previous models that assumed an incapacity of the cracked material to transmit forces.

Bazant and Oh [5] established a smeared crack model with the appearance of crack bands and the use of triaxial stress-strain relationships that allow a gradual softening of the material due to the microcracking process. The authors employed fracture mechanics concepts, and the properties of the cracked material are determined by three parameters: fracture energy, uniaxial limit strength, and the width of the crack band. With the popularization of smeared cracking models, many authors dedicated themselves to studying and comparing fixed and rotational cracking models and their applications. In this context, the works by Milford and Schnobrich [6], de Borst and Nauta [7], Rots et al. [8], and Rots and de Borst [9] can be mentioned.

More recently, some embedded crack models have emerged. They are used in the numerical simulation of cracking in reinforced concrete structures and are based on the insertion of discontinuities in the standard finite element. This model was used by Manzoli [10], who presented a study about the quality and the objectivity of the solutions obtained with different formulations of elements with strong discontinuity incorporated.

Over the years, several other papers were published proposing improvements in the crack models, different formulations for specific problems, and comparisons between models already established. In this context, the present paper aims to present a smeared crack model based on the inversion of the symmetrical compliance matrix. The model considers rotating smeared cracks whose direction is determined by the principal strain directions. Furthermore, it is expected to compare the behavior of the crack model with the use of four combinations of stress-strain relations proposed in the literature.

In order to evaluate the adopted model and validate the computational implementation, two examples were studied: an L-shaped panel and a three-point bending beam. In addition, the results obtained for the panel were compared with those presented by Winkler et al. [11] in their numerical and experimental study.

2 Numerical model

The smeared crack models consider that the discontinuity of the displacement field caused by the crack is distributed along the finite element. They are based on stress-strain relationships that consider the reduction of material stiffness from a given strain level, which directly impacts its physical properties. A shortcoming of this model is its difficulty in representing localized crack problems.

The numerical model adopted for the analysis of concrete structures is based on a smeared crack model that uses a local secant constitutive matrix obtained from the inverse of the symmetric compliance matrix for plane stress problems. Furthermore, the mechanical behaviour of concrete is defined by constitutive stress-strain relations that are able to compute the degradation of its physical properties. In this paper were used the relationships proposed by Boone and Ingraffea [12], Carreira and Chu [13], Carreira and Chu [14] e Kaklauskas [15].

2.1 Smeared crack model

The smeared crack model employed depends on the use of a local secant constitutive matrix that takes into account some material properties that are: the Young's modulus; the secant modulus in each of the principal directions in the current state of strain; the Poisson's ratio that is kept constant throughout the analysis; and the shear modulus. The development of this matrix will be described below, based on what was exposed in the thesis of Penna [16].

First, the relationship presented in eq. (1) must be considered, which associates the stress tensor in Voigt notation $\boldsymbol{\sigma}_l$ and the strain tensor in Voigt notation ϵ_l, both in a local coordinate system, here oriented in the principal strain directions, in terms of the secant compliance matrix $\mathbf{C}_l^s$.

$$\boldsymbol{\epsilon}_l = \mathbf{C}_l^s \boldsymbol{\sigma}_l. \tag{1}$$

Considering a orthotropic material and a symmetrization process, the compliance matrix $\mathbf{C}_l^s$ for plane stress problems is given by eq. (2):

$$\mathbf{C}_l^s = \begin{bmatrix} \dfrac{1}{E_1} & -\dfrac{\nu}{E_0} & 0 \\ -\dfrac{\nu}{E_0} & \dfrac{1}{E_2} & 0 \\ 0 & 0 & \frac{1}{G_{12}} \end{bmatrix}, \tag{2}$$

where ν is the material Poisson's ratio, E_0 is the Young's modulus, E_1 and E_2 are the material secant modulus in the principal strain directions and G_{12} is the shear modulus that are calculated by eq. (3):

$$G_{12} = \frac{E_0 E_1 E_2}{E_0 E_1 + E_0 E_2 + 2\nu E_1 E_2}. \tag{3}$$

The inverse of the compliance matrix presented in eq. (2) is the local secant constitutive matrix $\mathbf{D}_l^s$ shown in eq. (4) which considers a residual transverse stiffness due to the friction between the crack faces.

$$\mathbf{D}_l^s = \frac{1}{1 - \dfrac{E_1 E_2}{E_0^2}\nu^2} \begin{bmatrix} E_1 & \dfrac{\nu E_1 E_2}{E_0} & 0 \\ \dfrac{\nu E_1 E_2}{E_0} & E_2 & 0 \\ 0 & 0 & \left(1 - \dfrac{E_1 E_2}{E_0^2}\nu^2\right) G_{12} \end{bmatrix}. \tag{4}$$

The compliance matrix and the secant constitutive matrix given in eq. (2) and eq. (4) respectively, were obtained for the local system that is aligned with the directions of the principal strains. However, the constitutive matrix must also be obtained in the global system according to eq. (5).

$$\mathbf{D}_g^s = \mathbf{T}_\epsilon^T \mathbf{D}_l^s \mathbf{T}_\epsilon, \tag{5}$$

where $\mathbf{T}_\epsilon$ is the strain transformation matrix.

As the incremental-iterative nonlinear analysis process used is based on a tangent formulation, it is necessary to calculate the incremental tangent stiffness matrix that depends on the tangent constitutive matrix $\mathbf{D}_g^t$ in the global coordinate system. Such a matrix can be determined from eq. (6):

$$\mathbf{D}_g^t = \mathbf{T}_\epsilon^T \mathbf{D}_l^t \mathbf{T}_\epsilon + \frac{\partial \mathbf{T}_\epsilon^T}{\partial \boldsymbol{\epsilon}_g} \boldsymbol{\sigma}_l, \tag{6}$$

where the parcel $\dfrac{\partial \mathbf{T}_\epsilon^T}{\partial \boldsymbol{\epsilon}_g} \boldsymbol{\sigma}_l$ expresses the influence of possible changes in the transformation matrix $\mathbf{T}_\epsilon$ during the iterative-incremental process, $\boldsymbol{\epsilon}_g$ represents the strains in the global coordinate system and $\mathbf{D}_l^t$ is the local tangent constitutive matrix that it is determined by eq. (7):

$$\mathbf{D}_l^t = \mathbf{D}_l^s + \frac{\partial \mathbf{D}_l^s}{\partial \boldsymbol{\epsilon}_l} \boldsymbol{\epsilon}_l. \tag{7}$$

Both secant and tangent constitutive matrices depend on the values of secant and tangent modulus in the principal strain directions for monitoring the material damage process. These values depend on the current state of deformations and, therefore, can be obtained from stress-strain laws.

2.2 Stress-strain relationship of concrete

Over the years, many authors have proposed stress-strain relationships that describe the mechanical behavior of concrete. These relationships were derived from mathematical equations that models experimental results and are fundamental for the application of smeared crack models.

Following will be presented the stress-strain relationships studied in this work and in the analysis they will be combined with each other. The nomenclature used in the equations can be summarized by: E_0 is the Young's modulus, σ_t and σ_c are the principal tensile and compressive stresses, respectively, ϵ is the principal current strain, f_t is the tensile strength and ϵ_t its corresponding strain, f_c is the concrete strength and ϵ_c its corresponding strain, h_c is the characteristic length and G_f is the fracture energy by crack length.

Relationship proposed by Carreira and Chu [13] and Carreira and Chu [14]

Carreira and Chu [13] presented a polynomial equation to represent the stress-strain behavior of plain concrete in compression. The law is defined by physical parameters such as the stress and strain limits of the material. Both the ascending and descending branches fit data obtained from different testing conditions. Later, Carreira and Chu [14] proposed the use of the same polynomial equation to represent the behavior of reinforced concrete in tension and the proposed equation will also be used in this work to simulate the behavior of concrete without reinforcement. The proposed relationship, applied for both tension and compression, is given by the eq. (8):

$$\sigma_i = f_i \frac{k\left(\dfrac{\epsilon}{\epsilon_i}\right)}{k-1+\left(\dfrac{\epsilon}{\epsilon_i}\right)^k}, \qquad \text{with } k = \frac{1}{1-\left(\dfrac{f_i}{\epsilon_i E_0}\right)}, \qquad \text{where } i = t, c, \qquad \text{and } \epsilon_i > \frac{f_i}{E_0}. \tag{8}$$

Relationship proposed by Boone and Ingraffea [12]

Boone and Ingraffea [12] proposed a stress-strain law representing the behavior of concrete in tension. The formula, based on fracture energy and stress and strain limits, is given by eq. (9) and is valid in the description of the descending branch of the stress-strain curve, the ascending part being considered linear.

$$\sigma_t = f_t e^{-k(\epsilon-\epsilon_t)}, \qquad \text{with } k = \frac{h_c f_t}{G_f}. \tag{9}$$

Relationship proposed by Kaklauskas [15]

Kaklauskas [15] presents a relationship for concrete in compression based on tests carried out on concrete beams and slabs. This relationship is presented in eq. (10):

$$\sigma_c = f_c \left[2\frac{\epsilon}{\epsilon_c} - \left(\frac{\epsilon}{\epsilon_c}\right)^2\right], \qquad \text{with } \epsilon_c = \frac{2f_c}{E_0}. \tag{10}$$

Representation of the stress-strain curves

Figure 1a brings representations of the stress-strain curves proposed by Carreira and Chu [14] and by Boone and Ingraffea [12] for tensile stresses, considering different values of f_t, while Fig. 1b shows different curves produced from the relationship proposed by Carreira and Chu [13] and by Kaklauskas [15] for compressive stresses.

3 Numerical examples

The smeared crack model described before was applied to two classic examples involving concrete structures and the results obtained will now be presented.

3.1 L-shaped panel

The first example studied deals with an L-shaped concrete panel with its base clamped. The structure is subjected to a vertical distributed loading q along its left edge. The mesh is formed by 300 square elements with four nodes and initial dimension (0.025 x 0.025)m. Details of the panel's geometry and mesh can be seen in Fig. 2a. For all simulations with this structure were adopted: $E_0 = 25850$ MPa, $\nu = 0.18$, iterative method tolerance equals to 10^{-4} and 300 incremental steps.

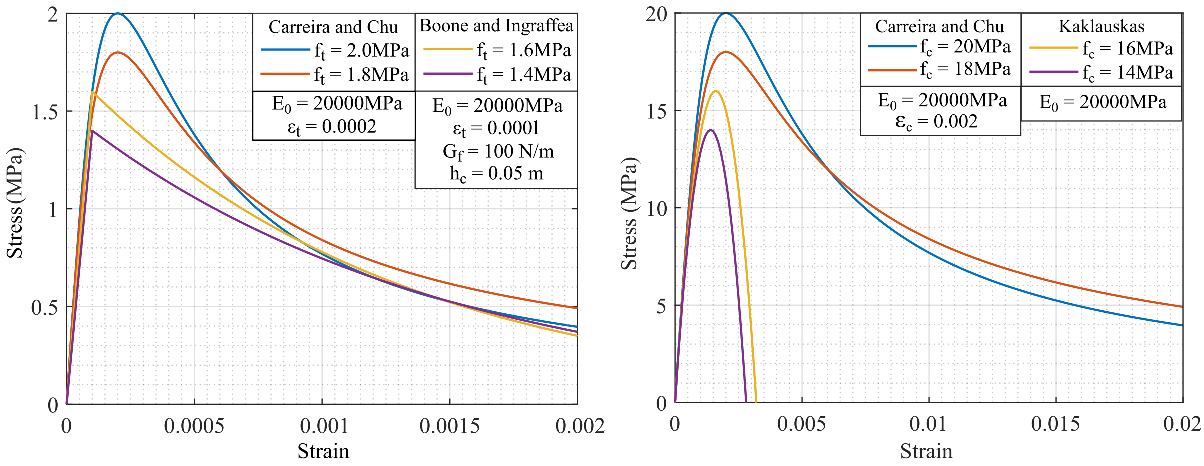

(a) Curves for concrete in tension

(b) Curves for concrete in compression

Figure 1. Stress-strain curves

3.2 Three-point bending beam

The second example analyzes a simply supported concrete beam subjected to a concentrated load P in its vertical symmetry axis, where this has a geometric discontinuity. The mesh is formed by 3980 square elements with four nodes and initial dimension (0.01 x 0.01)m. Details of the beam geometry, its measurements and mesh, is presented in Fig. 2b. For all simulations with this structure were adopted: $E_0 = 30000$ MPa, $\nu = 0.2$, iterative method tolerance equals to 10^{-4} and 150 incremental steps.

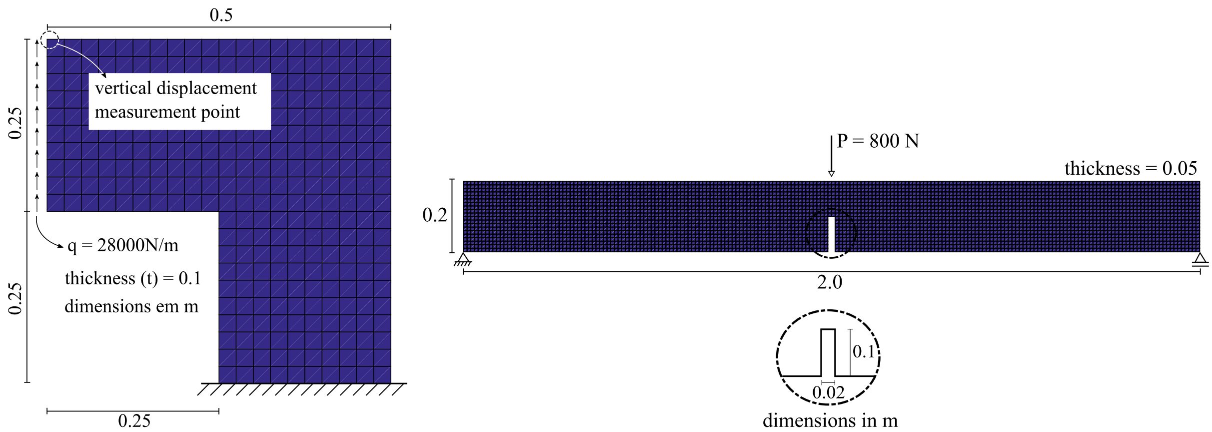

(a) L-shaped panel

(b) Three-point bending beam

Figure 2. Geometry and mesh for the structural models

3.3 Analysis of the results

For the panel the values assigned for each parameter of the stress-strain laws was: $f_c = 31$ MPa, $\epsilon_c = 0.0022$, $f_t = 2.7$ MPa, $\epsilon_t = 0.0001925$ for the relationship proposed by Carreira and Chu [14] and $\epsilon_t = 0.00010445$ for the relationship proposed by Boone and Ingraffea [12], $h_c = 28$ mm, $G_f = 0.065$ N/mm. And for the beam it was assumed that: $f_c = 33.3$ MPa, $\epsilon_c = 0.002$, $f_t = 3.3$ MPa, $\epsilon_t = 0.00022$ for the relationship proposed by Carreira and Chu [14] and $\epsilon_t = 0.00011$ for the relationship proposed by Boone and Ingraffea [12], $h_c = 40$ mm, $G_f = 0.124$ N/mm. It is noteworthy that, to obtain the equilibrium trajectory in both examples, it was used the standard Newton-Raphson method with the generalized displacement control method as a method of solving the system of nonlinear equations.

The results obtained for the L-shaped panel were compared with those found by Winkler et al. [11] in their numerical and experimental studies. Such comparison is presented in Fig. 3, where can been seen good agreement between the results. It is noticed a very similar behavior of the equilibrium curves and more accentuated differences in relation to the maximum load reached by the smeared crack model, which is lower than that observed by Winkler et al. [11].

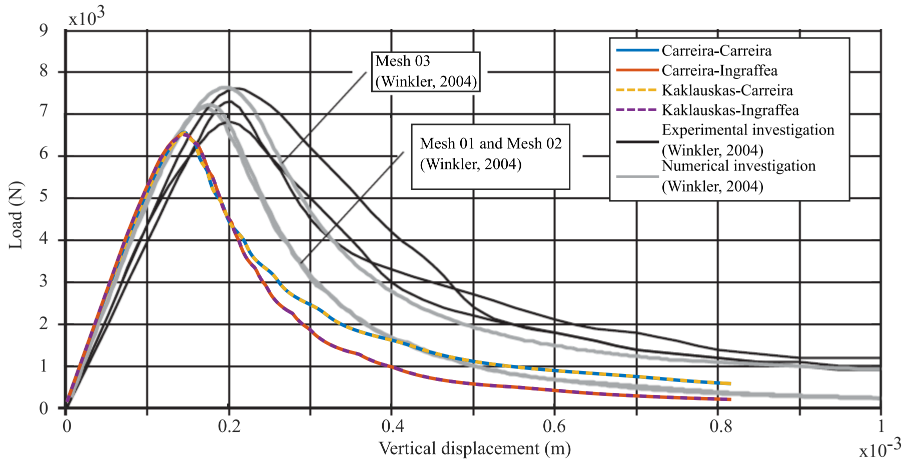

Figure 3. Validation of results for the L-shaped panel

The results for the beam are shown in Fig. 4. The equilibrium curves obtained for each of the adopted stress-strain relationships are very similar with more visible differences in the post-critical regime of the material.

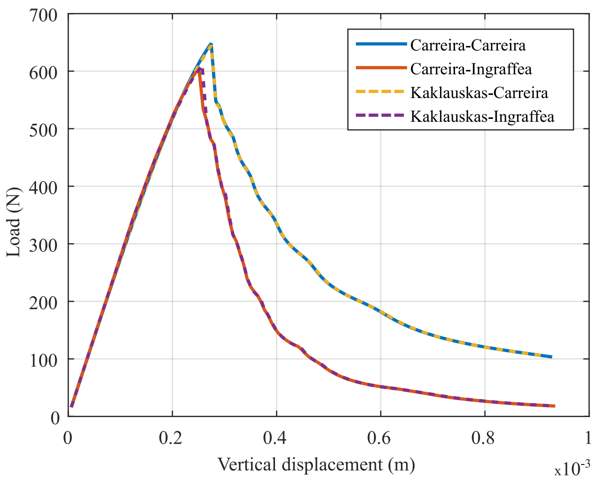

Figure 4. Equilibrium curves for three-point bending beam

As in the previous example, it can been seen a grouping of the equilibrium curves where the concrete tensile behavior is represented by the equation given by Carreira and Chu [14] and those in which such behavior is governed by the formulation proposed by Boone and Ingraffea [12]. As the tensile strength of concrete is considerably lower than its compressive strength, for the cracking process, the concrete tensile behavior is more relevant, and therefore the choice of the relationship governing this behavior has more influence in the results. The difference between the curves can be explained by the fact that the relationship proposed by Boone and Ingraffea [12], in addition to the stress and strain elastic limits, also considers the fracture energy per crack length G_f. This parameter makes it difficult to make an exact match of stress-strain relationship proposed by Boone and Ingraffea [12] with that one proposed by Carreira and Chu [14]. As the same Young's modulus was adopted for both, the differences in the linear elastic regime are very small.

4 Conclusions

The studied smeared cracking model is easy to understand and to implement and it was successfully used in the analysis of two concrete structural models. The results obtained are in accordance with patterns found in the literature and are able to represent the behavior of the structure in the linear elastic regime and in the post-critical regime. The use of different stress-strain laws to represent the material behavior does not significantly interfere in the results found, being only necessary an adjustment of the values of the input parameters according to the data available for a given structure.

Acknowledgements. The authors gratefully acknowledge the agencies CAPES (Coordination for the Improvement of Higher Education Personnel, PROCAD 88881.068530/2014-0), FAPEMIG (Minas Gerais Research Foundation, project PPM-00106-17), CNPq (National Council for Scientific and Technological Development, project 311576/2018-4-PQ), UFJF (Federal University of Juiz de Fora, grant PBPG - ID705).

Authorship statement. The authors hereby confirm that they are the sole liable persons responsible for the authorship of this work, and that all material that has been herein included as part of the present paper is either the property (and authorship) of the authors, or has the permission of the owners to be included here.

References

[1] D. Ngo and A. C. Scordelis. Finite element analysis of reinforced concrete beams. *American Concrete Institute Journal*, vol. 67, pp. 152–163, 1967.
[2] O. L. Manzoli, M. A. Maedo, L. A. G. Bitencourt Jr., and E. A. Rodrigues. On the use of finite elements with a high aspect ratio for modeling cracks in quasi-brittle materials. *Engineering Fracture Mechanics*, vol. 153, pp. 151–170, 2016.
[3] Y. L. Rashid. Ultimate strength analysis of prestressed concrete pressure vessels. *Nuclear Engineering and Design*, vol. 7, pp. 334–344, 1968.
[4] M. Suidan and W. C. Schnobrich. Finite element analysis of reinforced concrete. *Journal of the Structural Division*, vol. 99, n. 10, pp. 2109–2121, 1973.
[5] Z. P. Bazant and B. Oh. Crack band theory for fracture of concrete. *Matériaux et Construction*, vol. 16, n. 3, pp. 155–177, 1983.
[6] R. V. Milford and W. C. Schnobrich. The application of the rotating crack model to the analysis of reinforced concrete shells. *Computers and Structures*, vol. 20, n. 1-3, pp. 225–234, 1985.
[7] de R. Borst and P. Nauta. Non-orthogonal cracks in a smeared finite element model. *Engineering Computations*, vol. 2, pp. 35–46, 1985.
[8] J. G. Rots, P. Nauta, G. M. A. Kusters, and J. Blaaunwendraad. Smeared crack approach and fracture localization in concrete. *HERON*, vol. 30, n. 1, pp. 1–48, 1985.
[9] J. G. Rots and de R. Borst. Analysis of mixed-mode fracture in concrete. *Journal of Engineering Mechanics*, vol. 113, n. 11, pp. 1739–1758, 1987.
[10] O. L. Manzoli. Prediction of crack propagation via local constitutive models with a scheme to track the discontinuity path. *Revista Internacional de Métodos Numéricos para Cálculo y Diseño en Ingeniería*, vol. 27(3), pp. 180–188, 2011.
[11] B. Winkler, G. Hofstetter, and H. Lehar. Application of a constitutive model for concrete to the analysis of a precast segmental tunnel lining. *International Journal for Numerical and Analytical Methods in Geomechanics*, vol. 28, pp. 797–819, 2004.
[12] T. Boone and A. R. Ingraffea. Simulation of the fracture process at rock interface. *Proceedings of the fourth international conference in Numerical Methods in Fracture Mechanics*, vol. , pp. 519–531, 1987.
[13] D. J. Carreira and K. H. Chu. Stress-strain relationship for plain concrete in compression. *American Concrete Institute Journal*, vol. 82 (6), pp. 797–804, 1985.
[14] D. J. Carreira and K. H. Chu. Stress-strain relationship for reinforced concrete in tension. *American Concrete Institute Journal*, vol. 83 (1), pp. 21–28, 1986.
[15] G. Kaklauskas. Average stress-strain relations for concrete from experimental moment-strain diagrams of beams and slabs. *Journal of Civil Engineering and Management*, vol. 4, n. 2, pp. 92–100, 1998.
[16] S. S. Penna. *Formulação multipotencial para modelos de degradação elástica: unificação teórica, proposta de novo modelo, implementação computacional e modelagens de estruturas de concreto*. PhD thesis, Federal University of Minas Gerais, Graduation Program of Structural Engineering, Belo Horizonte, Brazil, 2011.